



## Acute toxicity of doxorubicin on isolated perfused heart: response of kinases regulating energy supply

Malgorzata Tokarska-Schlattner, Michael Zaugg, Rafaela da Silva, Eliana Lucchinetti, Marcus C. Schaub, Theo Wallimann and Uwe Schlattner

*AJP - Heart* 289:37-47, 2005. First published Mar 11, 2005; doi:10.1152/ajpheart.01057.2004

### You might find this additional information useful...

---

This article cites 54 articles, 25 of which you can access free at:

<http://ajpheart.physiology.org/cgi/content/full/289/1/H37#BIBL>

Updated information and services including high-resolution figures, can be found at:

<http://ajpheart.physiology.org/cgi/content/full/289/1/H37>

Additional material and information about *AJP - Heart and Circulatory Physiology* can be found at:

<http://www.the-aps.org/publications/ajpheart>

---

This information is current as of September 26, 2005 .



## Acute toxicity of doxorubicin on isolated perfused heart: response of kinases regulating energy supply

Malgorzata Tokarska-Schlattner,<sup>1,\*</sup> Michael Zaugg,<sup>2,3,\*</sup> Rafaela da Silva,<sup>2,3</sup>  
Eliana Lucchinetti,<sup>2,3</sup> Marcus C. Schaub,<sup>2</sup> Theo Wallimann,<sup>1</sup> and Uwe Schlattner<sup>1</sup>

<sup>1</sup>Institute of Cell Biology, Swiss Federal Institute of Technology, <sup>2</sup>Institute of Pharmacology and Toxicology, University of Zürich, and <sup>3</sup>Institute of Anesthesiology, University Hospital of Zürich, Zürich, Switzerland

Submitted 14 October 2004; accepted in final form 5 March 2005

**Schlattner, Malgorzata Tokarska, Michael Zaugg, Rafaela da Silva, Eliana Lucchinetti, Marcus C. Schaub, Theo Wallimann, and Uwe Schlattner.** Acute toxicity of doxorubicin on isolated perfused heart: response of kinases regulating energy supply. *Am J Physiol Heart Circ Physiol* 289: H37–H47, 2005. First published March 11, 2005; doi:10.1152/ajpheart.01057.2004.—Doxorubicin (DXR) is a widely used and efficient anticancer drug. However, its application is limited by the risk of severe cardiotoxicity. Impairment of cardiac high-energy phosphate homeostasis is an important manifestation of both acute and chronic DXR cardiotoxic action. Using the Langendorff model of the perfused rat heart, we characterized the acute effects of 1-h perfusion with 2 or 20  $\mu\text{M}$  DXR on two key kinases in cardiac energy metabolism, creatine kinase (CK) and AMP-activated protein kinase (AMPK), and related them to functional responses of the perfused heart and structural integrity of the contractile apparatus as well as drug accumulation in cardiomyocytes. DXR-induced changes in CK were dependent on the isoenzyme, with a shift in protein levels of cytosolic isoenzymes from muscle-type CK to brain-type CK, and a destabilization of octamers of the mitochondrial isoenzyme (sarcomeric mitochondrial CK) accompanied by drug accumulation in mitochondria. Interestingly, DXR rapidly reduced the protein level and phosphorylation of AMPK as well as phosphorylation of its target, acetyl-CoA-carboxylase. AMPK was strongly affected already at 2  $\mu\text{M}$  DXR, even before substantial cardiac dysfunction occurred. Impairment of CK isoenzymes was mostly moderate but became significant at 20  $\mu\text{M}$  DXR. Only at 2  $\mu\text{M}$  DXR did upregulation of brain-type CK compensate for inactivation of other isoenzymes. These results suggest that an impairment of kinase systems regulating cellular energy homeostasis is involved in the development of DXR cardiotoxicity.

creatine kinase; adenosine 5'-monophosphate-activated protein kinase; anthracyclines; cardiac energetics; cardiotoxicity

DOXORUBICIN (DXR) is a widely used and very efficient anticancer drug. However, its administration is limited by the risk of severe cardiotoxicity (31, 41). An important manifestation of DXR cardiotoxicity is an impaired cardiac high-energy phosphate metabolism. Acute and chronic consequences of DXR administration include compromised mitochondrial functions, such as respiration and generation of high-energy phosphates (30) and lowered phosphocreatine-to-creatine (PCr/Cr), PCr-to-ATP (PCr/ATP), and ATP-to-ADP (ATP/ADP) ratios as well as compromised calcium homeostasis (8, 29, 31). However, the involved molecular mechanisms are not yet entirely understood.

\* M. Tokarska-Schlattner and M. Zaugg contributed equally to this work.

Address for reprint requests and other correspondence: U. Schlattner, Institute of Cell Biology, Swiss Federal Institute of Technology, Hönggerberg HPM F23, CH-8093 Zürich, Switzerland (E-mail: schlattn@cell.biol.ethz.ch).

The maintenance of stable concentrations of myocardial high-energy phosphates, ATP, and PCr is a fundamental principle in the vertebrate heart. The PCr/ATP ratio is constant across species, as well as within a species, over a wide range of physiological cardiac workloads (12). Different regulatory systems have evolved to control cellular energy production and utilization. A key player of this regulatory network is the concerted action of several kinase systems, in particular, the energy transfer and buffer system of creatine kinase (CK) isoenzymes and the energy sensor AMP-activated protein kinase (AMPK) (4, 11, 28).

Cells and tissues with high or fluctuating energy demands like the heart rely on Cr and CK isoenzymes to cope with high ATP requirements (46, 49). By catalyzing the reversible transfer of phosphoryl groups between ATP and Cr, CK stores the free energy of ATP in the form of PCr and, vice versa, uses PCr to replenish cellular ATP pools. CK isoenzymes are expressed in vertebrates as tissue-specific as well as compartment-specific species. Two cytosolic isoenzymes, muscle-type CK (MCK) and brain-type CK (BCK), as well as two mitochondrial isoenzymes (MtCK), sarcomeric MtCK (sMtCK) and ubiquitous MtCK, are encoded by separate nuclear genes. The heart expresses both cytosolic CK isoenzymes, with a prevalence of MCK. They form two homodimers (MM- and BBCK) and a heterodimer (MBCK). Heart mitochondria contain considerable amounts of sMtCK, which forms mainly octamers. The interplay between cytosolic and mitochondrial CK isoenzymes, together with high intracellular concentrations of easily diffusible Cr and PCr, provides a unique cellular energy buffer and energy transport system, known as the CK/PCr circuit (38, 46).

AMPK plays a key role as an energy sensor, signaling system, and regulator of cellular energy substrate utilization (4, 11, 28). AMPK is activated by a fall of the cellular energy state, in particular, the ATP/AMP and PCr/Cr ratios, and by phosphorylation via upstream kinases that are possibly linked to signaling pathways involving radical production (55). Activated AMPK triggers catabolic pathways that generate ATP, e.g., fatty acid oxidation and glycolysis, and downregulates ATP-consuming processes that are not essential for short-term cell survival, such as the synthesis of lipids, carbohydrates, and proteins (10). AMPK can induce adaptation of the energy metabolism through cellular signaling cascades, phosphorylation of metabolic key enzymes, and transcriptional regulation. Cross-talk between AMPK and CK has been postulated (34),

The costs of publication of this article were defrayed in part by the payment of page charges. The article must therefore be hereby marked "advertisement" in accordance with 18 U.S.C. Section 1734 solely to indicate this fact.

including activation of AMPK by falling PCr/Cr ratios and inhibition of CK by phosphorylation via AMPK. However, the molecular details and the relevance *in vivo* remain controversial (16).

The aim of this study was to assess the role of these two kinases in the functional response of the heart to DXR, with a focus on acute DXR effects at relatively low, clinically relevant concentrations. These include 2  $\mu\text{M}$  DXR, which corresponds to an average peak DXR plasma concentration after a standard bolus DXR injection (9, 31, 42), and 20  $\mu\text{M}$  DXR, which has been shown to elicit pronounced functional defects in the perfused heart (27, 33). Such a supraclinical dose can also give additional clues on chronic effects as occurring during long-term drug exposure. Toxic effects of DXR on CK isoenzymes have been previously studied to some extent in different models (5, 6, 26, 44). Here, we characterize the response of the entire CK isoenzyme system *in situ* in a model of the perfused rat heart, with an emphasis on sMtCK, which is important for the control of mitochondrial respiration in oxidative heart muscle (22) and has been recently shown to be particularly susceptible to anthracyclines *in vitro* (44). The AMPK signaling cascade, which is of prime importance for the cellular energy state, has never been studied in relation to DXR effects in the heart. However, it has been shown that DXR rapidly affects glucose uptake and fatty acids oxidation in cultured cardiomyocytes (2, 14). Because both processes are also controlled by AMPK (16), these data suggest an interference of the drug with AMPK signaling. We took advantage of the perfused heart model to analyze simultaneously the effects of DXR on CK isoenzymes and AMPK and to relate these effects to cardiac functional responses. We show that DXR compromises myocardial energy metabolism by 1) a gradual impairment of the CK energy buffering and transport system, which has, however, a compensatory potential at low DXR doses; and 2) a rapid and strong downregulation of the AMPK energy sensing and regulating pathway. These results are not only relevant for the examined acute DXR effects but also for chronic DXR cardiotoxicity.

## MATERIALS AND METHODS

**Chemicals.** DXR hydrochloride was a kind gift of Pharmacia (Milan, Italy) or purchased from Fluka (Buchs, Switzerland). Stock solutions of DXR at 10 mM were prepared in water, aliquoted, and kept frozen until use. Further dilutions were made in Krebs-Henseleit solution directly before heart perfusion. Primary antibodies against CK isoenzymes have been generated and characterized previously in our laboratory (39); other primary antibodies were commercial, including polyclonal anti- $\alpha$ -AMPK (Cell Signaling), anti-phospho-(Thr<sup>172</sup>)- $\alpha$ -AMPK (Cell Signaling), anti-acetyl-CoA carboxylase- $\alpha$  (ACC- $\alpha$ ; Alpha Diagnostics), anti-phospho(Ser<sup>79</sup>)-ACC- $\alpha$  (Upstate), anti-active caspase 3 (Cell Signaling), anti-cleaved poly(ADP-ribose) polymerase (PARP; BD Biosciences Pharmingen), anti-heart myosin binding protein C (gift of J. C. Perriard, Swiss Federal Institute of Technology), anti-voltage-dependent anion channel 1 (VDAC1; Santa Cruz Biotechnology), and anti-GAPDH (Santa Cruz Biotechnology) as well as monoclonal anti-cytochrome *c* (BD Biosciences Pharmingen), anti-sarcomeric myosin heavy chain (A41025; DSHB), and anti- $\alpha$  sarcomeric actinin (Ea-53, Sigma). The disodium salts of ADP and NADP were obtained from Roche, PCr from Calbiochem, and P<sup>1</sup>P<sup>5</sup>-di(adenosine-5')-pentaphosphate pentasodium salt from Sigma. All other chemicals were at least of reagent grade.

**Perfusion protocol.** Hearts from decapitated and heparinized (500 U ip) male Wistar rats (300 g) were quickly removed and perfused in a noncirculating Langendorff apparatus with Krebs-Henseleit buffer containing 155 mM Na<sup>+</sup>, 5.6 mM K<sup>+</sup>, 138 mM Cl<sup>-</sup>, 2.1 mM Ca<sup>2+</sup>, 1.2 mM PO<sub>4</sub><sup>3-</sup>, 25 mM HCO<sub>3</sub><sup>-</sup>, 0.56 mM Mg<sup>2+</sup>, and 11 mM glucose. The buffer was saturated with 95% O<sub>2</sub>-5% CO<sub>2</sub> (pH 7.4, 37°C). Hearts were perfused at a constant pressure of 80 mmHg. A water-filled balloon-tipped catheter was inserted into the left ventricle through the left atrium. Left ventricular end-diastolic pressure (LVEDP) was adjusted to 0 mmHg at the end of the initial equilibration of 10 min. The volume of the balloon was not changed thereafter. The distal end of the catheter was connected to a performance analyzer (Plugsys Modular System, Hugo-Sachs; March-Hugstetten, Germany) using a pressure transducer. Perfusion pressure, epicardial electrocardiography, and left ventricular developed pressure (LVDP) [including the first derivatives of left ventricular pressure ( $\pm\text{dP}/\text{dt}$ )], and coronary flow (CF; Transit Time Flowmeter type 700, Hugo-Sachs) were recorded. All data were digitized and processed on a personal computer using the IsoHeart software (Hugo-Sachs). For each experimental group, four hearts were prepared, and functional parameters were recorded. The study was performed in accordance with the guidelines of the Animal Care and Use Committee of the University of Zurich.

**Cell fractionation and sample preparation.** Hearts were homogenized in ice-cold buffer containing 220 mM mannitol, 70 mM sucrose, 10 mM HEPES, 0.1% BSA, and 0.2 mM EDTA (pH 7.4). Aliquots of the homogenate were immediately frozen in liquid nitrogen and stored at -80°C; the remaining part was centrifuged at 700 g for 10 min at 4°C. The resulting supernatant was centrifuged at 7,000 g for 10 min at 4°C. The pellet obtained after the second centrifugation, representing a crude mitochondrial fraction, was resuspended in hypotonic phosphate buffer (10 mM sodium phosphate) at pH 9. The supernatant was kept as the soluble cytosolic fraction. Both were immediately aliquoted, frozen, and stored -80°C. If not stated otherwise, experiments were performed without the addition of any reducing agent to the heart samples in order not to counteract any DXR effects. For determination of total CK activity and sMtCK octamer/dimer analysis in mitochondrial fractions, samples were incubated with 100 mM sodium phosphate and 50 mM NaCl (final concentrations) (pH 9) for 1 h on ice. Protein concentrations were determined with the use of a BCA Protein Assay Reagent Kit (Pierce).

**CK enzymatic activity.** The reverse CK reaction (ATP production) was measured in a coupled photometric enzymatic assay as described by Schlattner et al. (37) with all reagents prepared without addition of  $\beta$ -mercaptoethanol ( $\beta$ -ME). Values were corrected for other ADP-consuming reactions (e.g., adenylate kinase) by subtracting activity measured in parallel in the absence of PCr. 1 U corresponds to 1  $\mu\text{M}$  of PCr transphosphorylated per min at pH 7.0 and 25°C.

**Cellulose polyacetate electrophoresis.** CK isoenzymes were separated by native cellulose polyacetate electrophoresis (CPAE) for 1 h at 150 V at room temperature (50). Subsequently, the CK bands were visualized by a color reaction coupled to the CK enzyme activity (47); the reaction mixture was supplemented with 100  $\mu\text{M}$  P<sup>1</sup>P<sup>5</sup>-di(adenosine-5')-pentaphosphate to inhibit interfering adenylate kinase activity. In some experiments, samples were treated for 1 h with substrates that form a transition state-analog complex (4 mM ADP, 5 mM MgCl<sub>2</sub>, 20 mM Cr, and 50 mM nitrate) to induce dissociation of sMtCK octamers into dimers.

**SDS-PAGE and immunoblotting.** Proteins separated by SDS-PAGE were semidry blotted onto polyvinylidene difluoride membranes (Immobilon-P, Millipore). In general, 20  $\mu\text{g}$  of protein were loaded on each lane. After being blocked, blots were immunostained with specific antibodies for 2 h at room temperature. The standard blocking buffer consisted of 4% milk, Tris-buffered saline (TBS), and 0.05% Tween 20 or of 5% milk, TBS, and 0.1% Tween 20 in the case of phospho- $\alpha$ -AMPK. The primary antibodies were diluted in corre-

sponding blocking buffer as follows: 1:100 for anti-GAPDH, 1:200 for anti-VDAC1, 1:500 for anti-ACC- $\alpha$  and anti-cytochrome *c*, 1:2,000 for anti-sarcomeric myosin heavy chain, 1:4,000 for cleaved PARP, and 1:1,000 for all other antibodies. Alternatively, for analysis of phospho- $\alpha$ -AMPK, overnight wet blotting at room temperature was applied; incubation with the primary antibodies was then performed also overnight at 4°C. Secondary peroxidase-coupled antibodies were diluted in blocking buffer at 1:2,000, and blots were incubated for 1 h at room temperature. Blots were developed with a Chemiluminescent Detection Kit (AppliChem). As a positive control for apoptotic markers, lysate of camptothecin-treated Jurkat cells (BD Biosciences Pharmingen) was used.

**Immunohistochemistry and fluorescence measurements.** In one experimental series, immunohistochemical analysis of control and anthracycline-treated heart tissue was performed. For this, at the end of the Langendorff protocol, hearts were embedded in OCT medium (Tissue-Tek, Sakura Finetek) and quickly frozen in liquid nitrogen. Heart cryosections of 10  $\mu$ m were fixed in 4% paraformaldehyde for 10 min at room temperature, blocked in 0.1 M glycine in PBS for 5 min, and then permeabilized in 0.2% Triton-PBS for 5 min. After sections were washed with PBS and blocked with 5% normal goat

serum for 30 min, they were incubated with primary antibodies overnight at 4°C. Anti-chicken heart myosin binding protein C was diluted at 1:100, anti- $\alpha$ -sarcomeric actinin was diluted at 1:500. After sections were washed in PBS for 10 min, secondary antibodies (1:500) were added for 1 h at room temperature. The specimens were further washed in PBS and mounted with anti-fading mounting medium (DAKO). Sections were examined using a Zeiss Axioplan 200 fluorescence microscope (Zeiss; Jena, Germany). DXR fluorescence in mitochondrial fractions was quantified with a fluorescence microplate reader (Gemini XS, Molecular Devices).

**Statistics.** For hemodynamic parameters, two-factor repeated-measures ANOVA was used to evaluate differences over time between groups ( $P < 0.05$  was considered statistically significant). Multiple paired *t*-tests were used to compare the parameters at each time point with the respective baseline measurements within groups, and unpaired *t*-tests were used to compare these parameters at each time point between groups. Post hoc Bonferroni tests for multiple comparisons were performed to determine statistical significance. Analyses were performed using SigmaStat (SPSS; Chicago, IL). For analysis of CK enzyme activity and band intensities in CPAE and immunoblots, the calculations of means, standard deviations, and statistical proba-

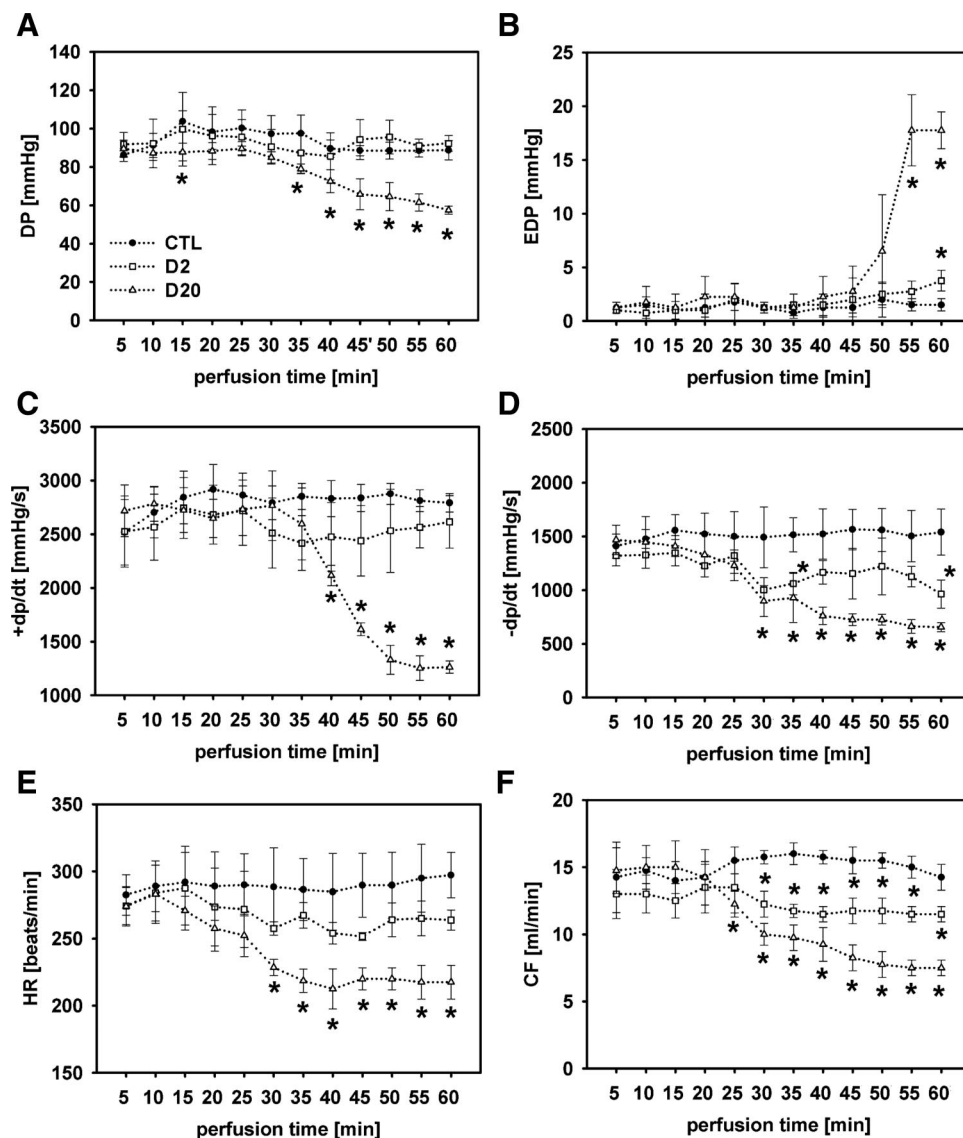


Fig. 1. Effect of doxorubicin (DXR) on myocardial function in isolated rat hearts. Isolated rat hearts were perfused with Krebs-Henseleit solution [control (CTL)] or Krebs-Henseleit solution containing DXR at concentrations of 2 (D2) and 20  $\mu$ M (D20) during 60 min according to the Langendorff method. A: developed pressure (DP); B: end-diastolic pressure (EDP); C: positive first derivative of left ventricular pressure (+dp/dt); D: negative first derivative of left ventricular pressure (-dp/dt); E: heart rate (HR); F: coronary flow (CF). Data are given as means  $\pm$  SD of 4 hearts at each time point. Significant differences from CTR (\* $P < 0.05$ ) are indicated.

Table 1. Percent changes in hemodynamic parameters in response to DXR

	LVDP	LVEDP	+dP/dt	-dP/dt	CF	HR	RPP
<i>30 min of DXR exposure (% of baseline)</i>							
CTR	113 (10)	100 (0)	111 (12)	106 (17)	113 (19)	101 (5)	106 (15)
DXR							
2 $\mu$ M	99 (5)	125 (50)	100 (10)	76 (8)*	96 (17)	94 (4)	90 (13)
20 $\mu$ M	95 (5)	100 (0)	102 (8)	62 (15)* $\ddagger$	68 (8)* $\ddagger$	86 (5)* $\ddagger$	79 (5)* $\ddagger$
<i>60 min of DXR exposure (% of baseline)</i>							
CTR	103 (3)	125 (50)	112 (11)	109 (9)	102 (12)	105 (2)	100 (8)
DXR							
2 $\mu$ M	101 (5)	375 (45)* $\ddagger$	105 (17)	73 (11)* $\ddagger$	90 (14)	96 (3)	94 (16)
20 $\mu$ M	64 (5)* $\ddagger$	1,550 (465)* $\ddagger$	47 (5)* $\ddagger$	44 (3)* $\ddagger$	51 (8)* $\ddagger$	79 (5)* $\ddagger$	50 (3)* $\ddagger$

Data are means (SD) and represent percentages of baseline values obtained after 10 min of stabilization;  $n = 4$  for each group. DXR, doxorubicin; CTR, control. LVDP, left ventricular (LV) developed pressure; LVEDP, LV end-diastolic pressure; +dP/dt, inotropy; -dP/dt, lusitropy; CF, coronary flow; HR, heart rate; RPP, rate-pressure product. \* $P < 0.05$  vs baseline (paired  $t$ -test);  $\ddagger P < 0.05$  vs. time-matched DXR (2  $\mu$ M) and vs. CTR, respectively (unpaired  $t$ -test);  $\ddagger P$  vs. time-matched CTR (unpaired  $t$ -test).

bility with Student's  $t$ -test ( $P < 0.05$  was considered statistically significant) were performed with Excel (Microsoft). Bands on CPAE and immunoblots were digitized and quantified with a 16-bit charge-coupled device camera-based Kodak imaging system.

## RESULTS

*DXR impairs myocardial function in a dose-dependent manner.* The effect of DXR on hemodynamic parameters of isolated rat hearts is summarized in Fig. 1 and Table 1. In control hearts, hemodynamic parameters, including LVDP, LVEDP, inotropy (+dP/dt), lusitropy (relaxation index, -dP/dt), CF, and HR were stable throughout the entire perfusion period of 60 min. DXR affected cardiac function in a dose-dependent manner. At a concentration of 2  $\mu$ M, the drug did not change LVDP and only marginally affected +dP/dt, CF, and HR. However, LVEDP and -dP/dt were significantly altered compared with baseline values. The relaxation index (-dP/dt), showing a detectable onset of decline already after 30 min of perfusion with 2  $\mu$ M DXR, appeared to be the most sensitive hemodynamic marker of acute DXR cardiotoxicity. In contrast, 20  $\mu$ M DXR had marked effects on all hemodynamic parameters. A 60-min perfusion period resulted in a 36% decrease in LVDP, a decrease of 53% in +dP/dt and of 56% in -dP/dt, a 49% decrease in CF, and a 21% decrease in HR. In accordance with the decreased CF, the rate-pressure product was markedly reduced after only 30 min of DXR perfusion at 20  $\mu$ M. The hemodynamic pattern of acute cardiac toxicity as observed at 20  $\mu$ M DXR is consistent with other reports based on the perfused heart model (27) as well as with the clinical picture that is characterized by arrhythmia, reversible hypotension, and pericarditis (18, 31).

*DXR accumulates in nuclei and mitochondria without affecting gross sarcomeric structure.* Immunostaining of heart tissue for  $\alpha$ -actinin, identifying Z-discs, and myosin-binding protein C indicated that the general myofibrillar structure remained intact under the DXR treatment (Fig. 2). Therefore, in contrast to what was found by others in DXR-treated cardiomyocytes (24), our experimental setup did not lead to myofibrillar disarray. Localization of the drug in cardiac cells was analyzed by confocal microscopy making use of red DXR autofluorescence (Fig. 3). Confocal images showed important DXR accumulation in nuclei already at 2  $\mu$ M (Fig. 3A) and,

mainly at 20  $\mu$ M DXR, an additional particulate fluorescence signal in the cell body that was reminiscent to mitochondria. Immunostaining for mitochondrial markers like cytochrome  $c$  oxidase or VDAC, however, elicited a red fluorescence endogenous to the cardiac tissue that masked the particulate DXR fluorescence signal (data not shown). Therefore, mitochondrial subfractions of cardiac tissue were used to determine mitochondrial DXR by fluorimetric analysis (Fig. 3B). These results confirmed a pronounced accumulation of the drug in heart mitochondria at 20  $\mu$ M DXR.

*DXR causes an isoenzyme shift in the CK protein pattern.* The amount of CK isoenzyme protein was analyzed by immunoblotting with isoenzyme-specific antibodies (Fig. 4). The semiquantitative data showed a differential effect of DXR on BCK and MCK protein abundance. Whereas BCK protein was significantly increased at both DXR concentrations, MCK protein decreased and reached significantly lower levels than control at 20  $\mu$ M DXR. This change, which is known as CK isoenzyme shift, could be observed here after only 1 h of perfusion and at very low DXR concentrations. The level of sMtCK protein was not significantly changed by DXR.

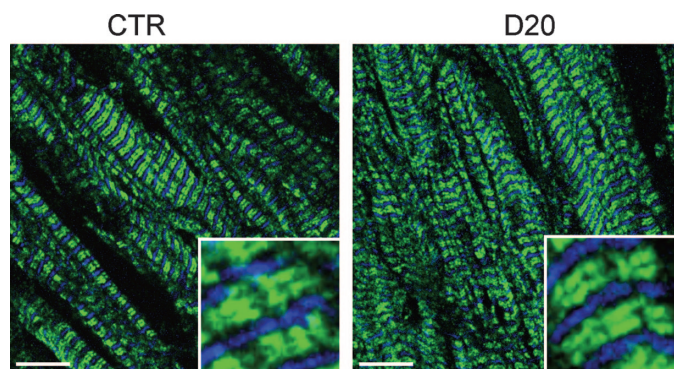


Fig. 2. Effect of DXR on myofibrillar structure. Immunofluorescence confocal microscopy images of typical 10- $\mu$ m sections from rat hearts perfused without (CTR) or with 20  $\mu$ M DXR are shown. Sections were stained for  $\alpha$ -actinin using Alexa 488-conjugated secondary antibody (blue channel) and for myosin-binding protein C using Cy5-conjugated secondary antibody (green channel). The insets show 4-fold magnification of a typical sector. Bars = 1  $\mu$ m. Note that there are no discernible differences in myofibrillar structure between CTR and DXR-perfused hearts.

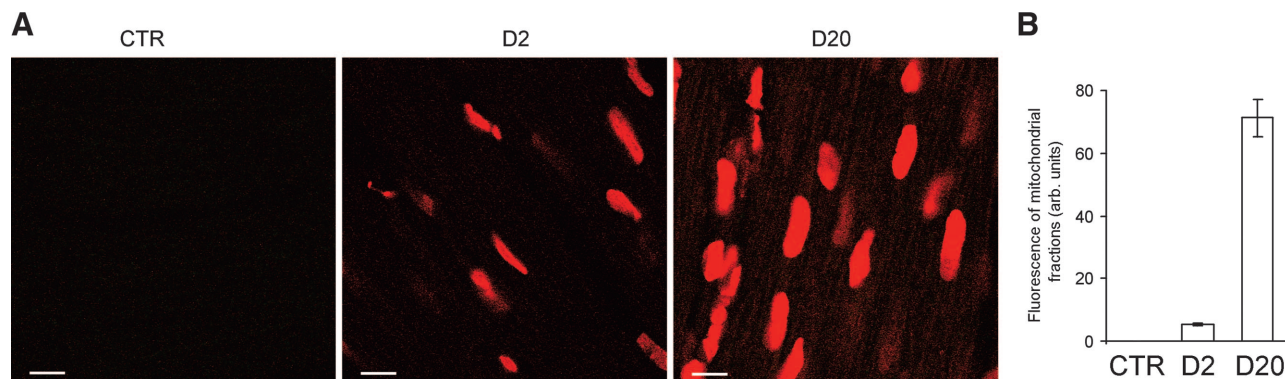


Fig. 3. Accumulation of DXR in nuclei and mitochondria. *A*: DXR distribution in cardiac cells analyzed with confocal microscopy. Images of typical 10- $\mu$ m sections of rat hearts perfused without (CTR) or with DXR at 2 or 20  $\mu$ M show DXR autofluorescence (red channel). Bars = 1  $\mu$ m. Note that DXR accumulates in nuclei already at 2  $\mu$ M; an additional particulate pattern becomes apparent at 20  $\mu$ M. *B*: DXR content in mitochondrial fractions of cardiac cells. DXR was quantified by its autofluorescence at 560 nm (excitation at 480 nm). Arb units, arbitrary units. Data are given as means  $\pm$  SD;  $n = 4$ . Note that DXR accumulation in mitochondria is apparent at 20  $\mu$ M DXR.

**Differential effects of DXR on CK isoenzyme activity.** Total CK activity of the rat heart was determined with a spectrophotometric assay. It remained unchanged after perfusion with 2  $\mu$ M DXR but decreased by about 20% after perfusion with 20  $\mu$ M DXR (Fig. 5). To analyze DXR effects on the activity of individual CK isoenzymes, heart homogenates were separated by native CPAE (Fig. 6). Total homogenates showed the typical isoenzyme pattern of the rat heart (46), consisting of four CK isoenzymes with predominating MMCK and sMtCK (Fig. 6A). DXR-induced changes could be quantified when loading and coloration reaction were adjusted for each isoenzyme separately (Fig. 6B). BBCK activity was significantly upregulated at 2  $\mu$ M DXR but returned to the control level at 20  $\mu$ M DXR. Because protein levels remain elevated at 20  $\mu$ M DXR (Fig. 4), this indicated BBCK inactivation. MBCK activity showed a trend to similar changes, which did, however, not reach significance. In contrast, enzymatic activity of MMCK decreased significantly at both DXR concentrations, in correlation with MCK protein levels. The octameric sMtCK that is detectable in nonreducing CPAE did not show any significant change in enzymatic activity. The relative contributions of individual isoenzymes to total CK activity were calculated separately (Fig. 6C). They showed that decreased MMCK activity at 2  $\mu$ M DXR is entirely compensated for by an increase in BBCK activity due to CK isoenzyme shift,

whereas compensation is lost at 20  $\mu$ M DXR, resulting in a net decrease of total CK activity.

**DXR destabilizes sMtCK octamers.** In contrast to dimeric cytosolic CK isoenzymes, mitochondrial isoenzymes occur as two interconvertible oligomeric species, dimers and octamers (38). The latter is predominant *in vivo* and is considered as the physiologically active species that binds to mitochondrial membranes and functions in cellular energy transduction (23). In both control and DXR-treated samples, sMtCK dimers were hardly detectable in CPAE performed under standard conditions (Figs. 6, *A* and *B*, and 7*A*, *left*). Here, any reducing agent like  $\beta$ -ME was omitted, because it could partially reverse the oxidative inactivation of sMtCK by DXR (44). However, when mitochondrial fractions were preincubated for 1 h with 20 mM  $\beta$ -ME or when recombinant sMtCK stored under reducing conditions were used, significant amounts of sMtCK dimer became detectable (Fig. 7*A*, *middle* and *right*). The addition of substrates forming a transition state-analog complex and known to trigger MtCK dimerization clearly showed that the reactivated species is the sMtCK dimer (Fig. 7*A*) (44). Thus, in contrast to homologous cytosolic CK, dimeric sMtCK is highly susceptible to inactivation under nonreducing conditions. The effect of DXR on the octamer-to-dimer ratio of sMtCK was therefore reevaluated in mitochondrial extracts pretreated with  $\beta$ -ME (Fig. 7*B*). A DXR concentration-dependent decrease of

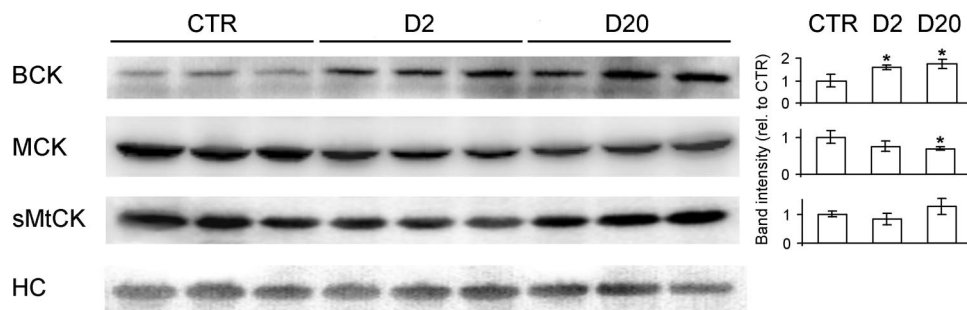


Fig. 4. Effect of DXR on protein level of creatine kinase (CK) isoenzymes. *Left*: SDS-PAGE immunoblots of homogenates from rat hearts perfused without (CTR) or with DXR at 2 or 20  $\mu$ M. Blots were probed for brain-type CK (BCK), muscle-type CK (MCK), and sarcomeric mitochondrial CK (sMtCK). *Right*: histograms show a quantification of band intensities relative to CTR and normalized to equal protein loading by probing and quantifying the same blots for sarcomeric myosin heavy chain (HC). Data are given as means  $\pm$  SD for 3 independent perfusion experiments. Significant differences from CTR ( $*P < 0.05$ ) are indicated.

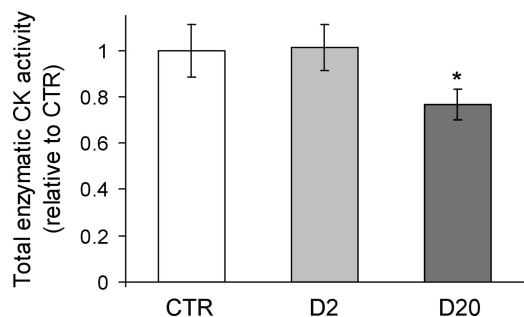


Fig. 5. Effect of DXR on total CK activity in isolated rat hearts. Enzymatic CK activities of rat heart perfused with 2  $\mu$ M (D2) or 20  $\mu$ M DXR (D20) relative to control hearts (CTR). CK activity was measured in total heart homogenates with a photometric coupled enzymatic assay for the reverse CK reaction (ATP production). Specific CK activity of control hearts was  $2.9 \pm 0.4$  U/mg total protein. Data are given as mean  $\pm$  SD of 4 hearts. \*Significantly different ( $P < 0.05$ ) from control.

the sMtCK octamer-to-dimer ratio was observed that was significant at 20  $\mu$ M DXR, in parallel with DXR accumulation in mitochondria (Fig. 3) and consistent with our previous in vitro study (44).

*DXR inhibits binding of sMtCK and cytochrome c to mitochondrial membranes.* An important property of MtCK is its high affinity to mitochondrial membranes, in particular to negatively charged cardiolipin (5, 40). DXR shows a similar high-affinity interaction with cardiolipin, which destabilizes mitochondrial membranes in general (e.g., via lipid oxidation) and competitively inhibits cardiolipin interaction of MtCK and cytochrome *c* (5, 43). Moreover, DXR can favor mitochondrial permeability transition that leads to cytochrome *c* release, a major trigger of apoptosis (53). To evaluate such effects in the DXR-perfused heart, we examined sMtCK and cytochrome *c* distribution in crude mitochondrial versus soluble (cytosolic) fractions (Fig. 8A). Perfusion with 20  $\mu$ M DXR significantly increased the amounts of sMtCK and cytochrome *c* in the soluble fraction, with solubilized sMtCK mainly consisting of dimeric species (data not shown). If this occurred in vivo, cytochrome *c* release should have triggered the apoptotic cascade. However, no increase of downstream apoptotic markers like activated caspase 3 and cleaved PARP was detectable in immunoblots of DXR-perfused heart samples at either 2 or 20  $\mu$ M DXR (Fig. 8B). Thus we conclude that 1-h perfusion with DXR had not yet activated the apoptotic cascade but rather sensitized mitochondrial membranes to rupture and to release sMtCK and cytochrome *c* during mitochondrial preparation.

*DXR interferes with the AMPK signaling cascade.* DXR impairs ATP production and, as suggested by the partial inactivation of CK isoenzymes, locally impairs PCr generation and ATP regeneration. According to Rajagopalan et al. (35), the production of free radicals should be significant under our experimental conditions (35). Because both stressors are known to activate AMPK, we examined the response of this energy-sensing kinase cascade to DXR. AMPK activation involves a dual mechanism with allosteric activation by AMP and covalent activation by phosphorylation at Thr<sup>172</sup> within the  $\alpha$ -subunit by specific upstream kinases (4). First, we used phosphosite-specific antibodies against phospho-Thr<sup>172</sup> to detect AMPK activation in control and DXR-treated hearts (Fig. 9). Considerable basal AMPK phosphorylation was observed

in control samples but was almost missing in samples treated with 2 or 20  $\mu$ M DXR. This significant decrease in phospho-AMPK signals was accompanied by a similar decrease in total AMPK protein except that the latter was less pronounced at 2

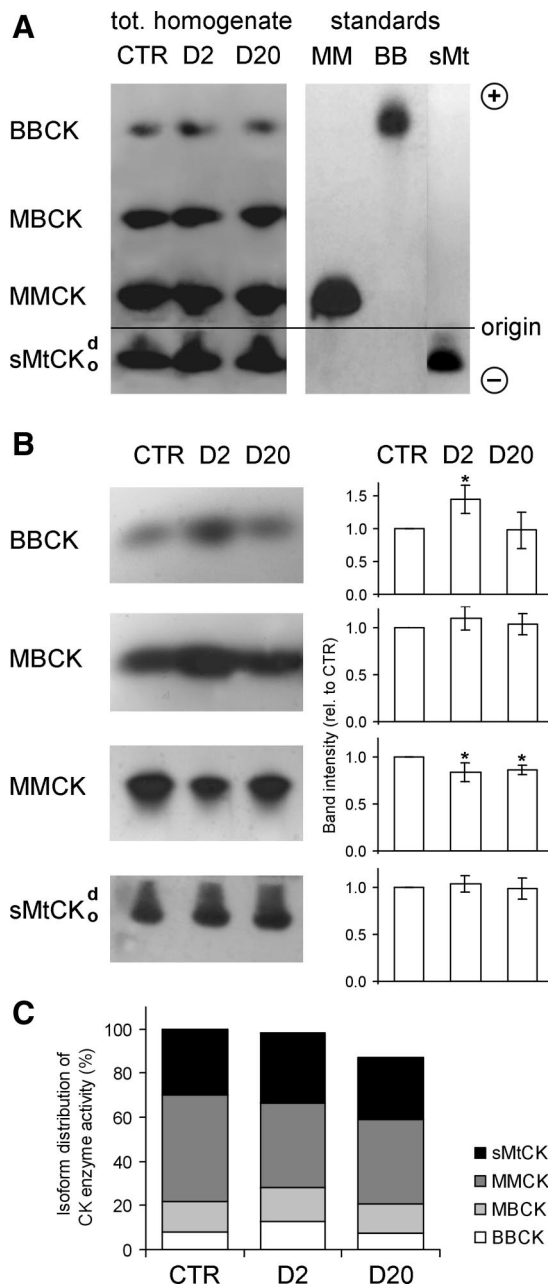


Fig. 6. Effect of DXR on the isoenzyme pattern of CK activity. CK isoenzymes from rat hearts perfused without (CTR) or with DXR at 2 or 20  $\mu$ M were separated by native cellulose polyacetate electrophoresis (CPAE) and detected by their enzymatic activity. Equal amounts of protein were loaded on each lane. *A*: typical CK activity patterns of homogenates. Purified rabbit MMCK and BBCK and recombinant human sMtCK were used as standards. d, sMtCK dimers; o, sMtCK octamers. *B*: CPAE separations of heart homogenates with optimized coloration of CK isoenzyme activities. One of three independent perfusion experiments is shown (*left*; see also MATERIALS AND METHODS). Histograms (*right*) show a quantification of band intensities relative to CTR. Data are given as means  $\pm$  SD;  $n = 3$ . Significant differences from CTR (\* $P < 0.05$ ) are indicated. *C*: relative contributions of CK isoenzymes to total CK activity in CTR and DXR-treated hearts calculated from band intensities assessed in *A* and *B*.

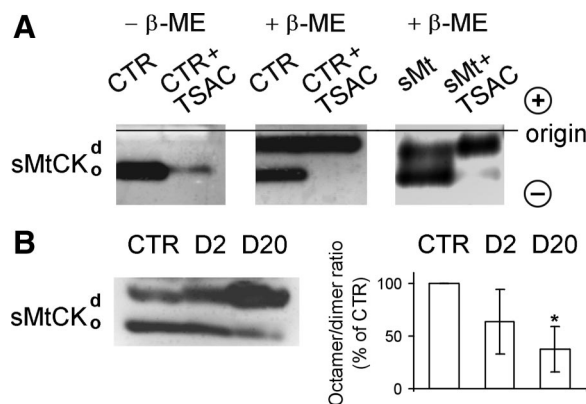


Fig. 7. Effect of DXR on the octamer-to-dimer ratio of sMtCK. Oligomeric species of sMtCK were separated by native CPAE and detected by their enzymatic activity. Equal amounts of protein were loaded on each lane. *A*: inactivation of dimeric sMtCK in mitochondrial fractions and reactivation by  $\beta$ -mercaptoethanol ( $\beta$ -ME). *Left*, CTR mitochondrial extract; *middle*, same extract preincubated with 20 mM  $\beta$ -ME for 1 h; *right*, recombinant human sMtCK kept in  $\beta$ -ME-containing storage buffer (consisting of octameric and dimeric species). Each sample was, in addition, treated for 1 h with substrates forming the transition state-analog complex (TSAC; see MATERIALS AND METHODS) to induce dissociation of sMtCK octamers into dimers. Note that sMtCK dimers are only visible (enzymatically active) in the presence of  $\beta$ -ME. *B*: octameric and dimeric sMtCK species in  $\beta$ -ME-pretreated mitochondrial extracts from rat hearts perfused without (CTR) or with DXR at 2 or 20  $\mu$ M. Representative data from 1 of 3 independent perfusion experiments are shown (*left*). The histogram (*right*) shows changes in the octamer-to-dimer ratio of sMtCK relative to CTR as calculated from band intensities. Data are given as means  $\pm$  SD;  $n = 3$ . \*Significantly different ( $P < 0.05$ ) from control.

$\mu$ M DXR, as revealed by general AMPK  $\alpha$ -subunit antibodies. We further compared this downregulation of AMPK, first described here, with the phosphorylation and protein level of ACC- $\alpha$ . The latter is an important downstream target of AMPK, whose phosphorylation gives a measure for both allosteric and covalent activation of AMPK and thus reflects the activity of the AMPK signaling pathway. Downregulation of AMPK was accompanied by a significant decrease in phosphorylated ACC- $\alpha$  at both DXR concentrations, whereas ACC- $\alpha$  protein remained largely unaffected. Thus the lack of covalent activation at AMPK-Thr<sup>172</sup> was not compensated by some other activation mechanism but indeed led to a partial shutdown of AMPK downstream signaling.

## DISCUSSION

This study, using a perfused rat heart model, demonstrates the susceptibility of the CK/PCr system and of the AMPK signaling pathway to DXR and their potential involvement in DXR cardiotoxicity. Despite a certain compensatory potential observed for CK, which involves an isoenzyme shift toward the more active BCK, the general toxicity limit of DXR is relatively low and close to clinical drug concentrations. Acute effects on both kinases were already observed at 2  $\mu$ M DXR, which corresponds to peak plasma concentrations in patients reaching 2–6  $\mu$ M DXR with a typical value of 1–2  $\mu$ M (9, 31, 42). At higher DXR concentrations of 10–20  $\mu$ M DXR, acute functional changes in the perfused heart become markedly pronounced as indicated by this and other studies (27, 33).

An important result of our detailed analysis of CK was an isoenzyme switch with decreased MCK and increased BCK

protein that was already apparent after 1 h and at the low dose of 2  $\mu$ M DXR and led to a fetal-like isoenzyme pattern. Basically, such an isoenzyme shift is known to occur in the heart under chronic pathological conditions, as, e.g., in hypertrophy, characterized by a compromised cellular energy state (15, 20, 45, 52). First, higher levels of BCK protein led to an increase in the enzymatic activity of BCK and MBCK, which may efficiently compensate for an inhibition of other CK isoenzymes, mainly MMCK. Second, an additional advantage of BCK upregulation may be the higher affinity for ADP and its higher specific activity (46, 49), possibly resulting in more efficient ATP regeneration. However, at the higher dose of 20  $\mu$ M DXR, BCK is also partially inactivated by DXR. It can no longer compensate for an activity loss of other CK isoenzymes, thus leading to a decrease in total CK activity by about 20%. The shift in the CK isoenzyme pattern could be due to rapid changes in gene expression, either because of specific susceptibility of CK genes to DXR (17) or because of a general induction of a fetal expression profile in response to stress (49, 51). Fast changes in gene expression after DXR exposure were already observed earlier (19). In addition, MMCK may be degraded or partially leak from DXR-treated cardiac cells (6, 13).

For sMtCK, no significant acute changes in either protein or activity level were observed, consistent with the results of Pelikan et al. (32). However, octamer stability and membrane binding of sMtCK were impaired, in particular at 20  $\mu$ M DXR. Both properties are equally important for the physiological roles of MtCK in energy channeling between mitochondria and cytosol (38) or inhibition of mitochondrial permeability transition (7), and failure of these functions may trigger apoptosis or necrosis. Similar to BCK inactivation, impairment of sMtCK at 20  $\mu$ M DXR occurred together with accumulation of the drug in cardiac mitochondria and clearly decreased cardiac function, consistent with an involvement of these isoenzymes in acute DXR cardiotoxicity. Mechanistically, as observed in our earlier in vitro study (44), accumulation of DXR at mitochondrial membranes rapidly affects sMtCK. DXR interaction with mitochondrial cardiolipin would competitively inhibit the binding of MtCK and other cardiolipin-interacting proteins like cytochrome *c*. Solubilization of sMtCK would make it a better substrate for oxidative modifications, which would trigger octamer dissociation into dimers that are even more susceptible to oxidative damage, thus entering a vicious cycle with progressive inactivation of sMtCK. However, such an accumulation of damage is expected to occur under chronic rather than acute DXR exposure.

Because activation of effector caspase 3 or cleavage of PARP was not detectable in DXR perfused hearts after 1 h, we have no evidence for apoptosis at this stage of treatment. This makes it rather unlikely that considerable amounts of cytochrome *c* were already released into the cytosol in situ. However, the presence of cytochrome *c* (and sMtCK) in the supernatant of extracts revealed that DXR had already sensitized mitochondrial membranes to become permeable, most likely during the isolation procedure. Therefore, in the long term, the DXR-treated heart could be more susceptible to apoptosis via mitochondrial permeability transition and cytochrome *c* release. This is consistent with a large body of evidence showing that DXR generates conditions known to trigger permeability transition in isolated mitochondria, like oxidative stress, lower

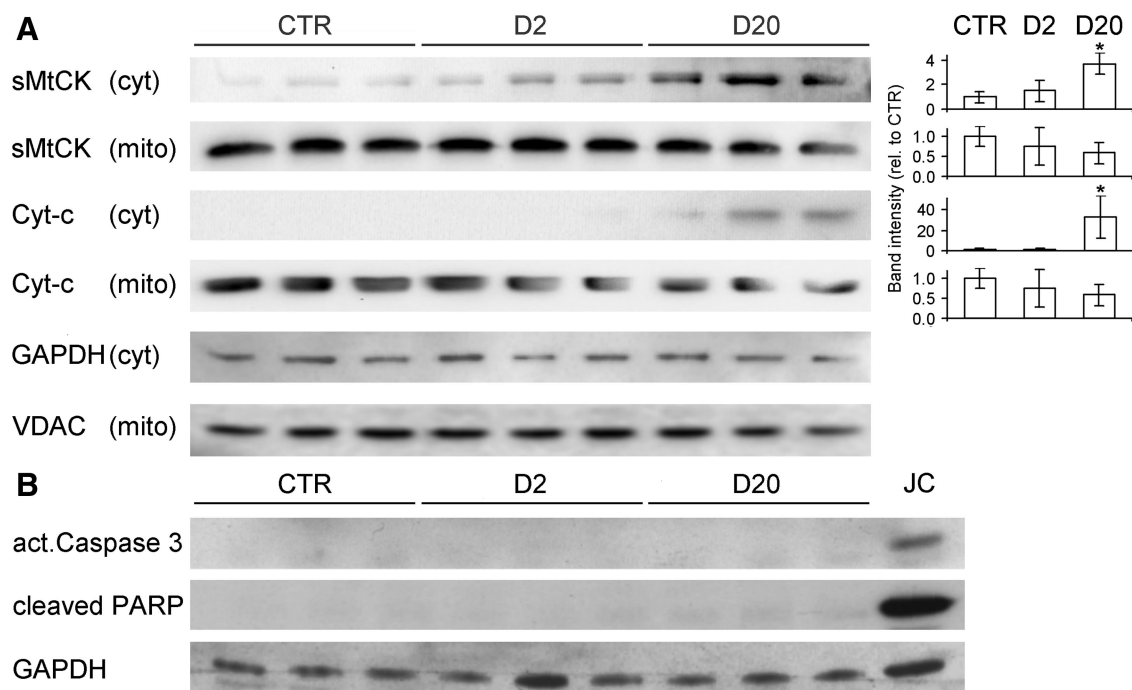


Fig. 8. Release of sMtCK and cytochrome *c* (Cyt-*c*) from mitochondria (*A*) without activation of the apoptotic cascade *in situ* (*B*). *A*: SDS-PAGE immunoblots (*left*) of cytosolic and mitochondrial fractions from rat hearts perfused without (CTR) or with DXR at 2 or 20  $\mu\text{M}$ . Blots were probed for sMtCK and Cyt-*c*. Histograms (*right*) show a quantification of band intensities relative to CTR and normalized to equal protein loading by probing and quantifying the same blots for GAPDH (cytosolic fraction) or voltage-dependent anion channel 1 (VDAC1; mitochondrial fraction). Data are given as means  $\pm$  SD for 3 independent perfusion experiments. Significant differences from CTR ( $*P < 0.05$ ) are indicated. *B*: immunoblots of total homogenates (20  $\mu\text{g}$  protein) from rat hearts perfused without (CTR) or with DXR at 2 or 20  $\mu\text{M}$  were probed for activated (act.) caspase 3 and cleaved poly(ADP-ribose) polymerase (PARP); lysate of camptothecin-treated Jurkat cells (JC; 15  $\mu\text{g}$  protein) was used as positive control. Equal protein loading was verified by probing the same blots for GAPDH.

ATP and calcium overload in the cytosol, decreased ability of mitochondria to accumulate calcium, and increased sensitivity to calcium-dependent mitochondrial membrane depolarization as well as changes in adenine nucleotide translocator function/expression (53). Similarly, other consequences of DXR treatment, like reduced membrane binding and dimerization of

sMtCK (7) or inhibition of BCK activity and AMPK signaling leading to impaired energy state would all be potentially proapoptotic in the long term.

AMPK was strongly impaired at both DXR concentrations. DXR rapidly reduced the level of total AMPK protein, accompanied by an even stronger decrease in the basic level of Thr<sup>172</sup>

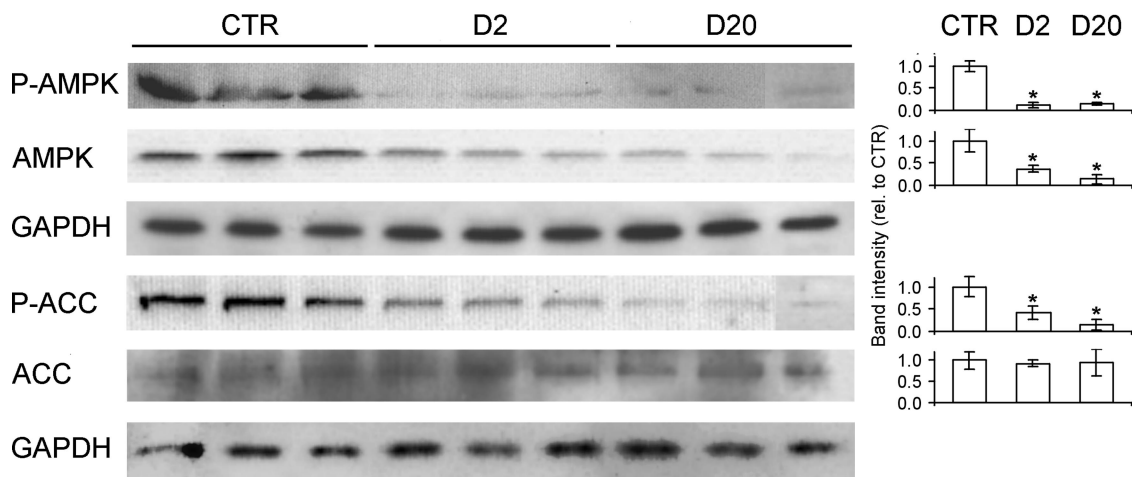


Fig. 9. Effect of DXR on phosphorylation and protein level of AMP-activated protein kinase (AMPK) and acetyl-CoA carboxylase (ACC). *Left*: SDS-PAGE immunoblots of total homogenates or cytosolic fractions from rat hearts perfused without (CTR) or with DXR at 2 or 20  $\mu\text{M}$ . Blots from homogenates were probed for AMPK phosphorylated at Thr<sup>172</sup> (P-AMPK) and  $\alpha$ -AMPK subunit protein (AMPK). Blots from cytosolic fractions were probed for phosphorylated ACC- $\alpha$  (P-ACC) and ACC- $\alpha$  protein (ACC). *Right*: histograms show a quantification of band intensities relative to CTR and normalized to equal protein loading by probing and quantifying the same blots for GAPDH. Data are given as means  $\pm$  SD for 3 independent perfusion experiments. Significant differences from CTR are indicated ( $*P < 0.05$ ).

phosphorylation, which is the activating phosphorylation due to upstream kinases like protein kinase LKB1 (4). These novel data indicate that indeed both AMPK protein and its basic activation state were decreased. Furthermore, the loss of active AMPK led to decreased phosphorylation of ACC- $\alpha$ , an AMPK downstream target, without affecting ACC- $\alpha$  protein levels. The latter underlines the susceptibility of AMPK protein to DXR. More importantly, the low phosphorylation of ACC- $\alpha$  not only shows the lack of covalent AMPK activation via phospho-Thr<sup>172</sup> but also the absence of any additional allosteric AMPK activation via a fall in ATP/AMP ratios. Thus in the DXR perfused heart, AMPK is not activated by some known AMPK trigger and is basically inactive. This is a rather unexpected result, because stress in general, and energetic or oxidative stress in particular, are known to impair cellular energy status and to rapidly activate AMPK for ATP generation (54). It seems that DXR generates deleterious conditions, which normally should activate AMPK (31, 48) but instead inhibit the beneficial stress response of the kinase, thus entering a vicious cycle that may be an important factor in drug toxicity. This failure of AMPK to react properly to oxidative or energetic stress may be an important mechanism contributing to drug toxicity, both in the heart and tumors. The mechanisms underlying inhibition of AMPK are not clear. Not much is known about the upstream signaling of this pathway in general. Because DXR does not directly affect the activity of recombinant AMPK in vitro (data not shown), alterations in gene expression and upstream signaling require further investigation.

To evaluate the importance of impaired CK and AMPK activities for anthracycline cardiotoxicity, we related these changes to structural and functional parameters of the perfused heart. Only few of the cardiac functional parameters were altered at 2  $\mu$ M DXR, whereas all of them were drastically affected at 20  $\mu$ M DXR, yet without any histologically visible damage of the myocardial contractile apparatus. Because changes in the CK system were moderate at both DXR concentrations, they are not likely to be a main factor for the substantial cardiac dysfunction seen at 20  $\mu$ M DXR. However, the lower total CK activity together with solubilized and dimerized sMtCK could certainly contribute to a diminished high-energy phosphate level. For example, 1-h perfusion of rat hearts with 10  $\mu$ M DXR was estimated to cause an about 20% decrease in both ATP and PCr levels (33, 40), and a similar decrease was observed in animals upon single DXR injection (29). In turn, it seems plausible that decreased AMPK signaling can be an important factor mediating acute cardiac dysfunction, especially under hypoxic conditions due to strongly decreasing coronary flow, as it was the case at 20  $\mu$ M DXR. Recently, Russell and co-workers (36) have shown that transgenic mice expressing dominant negative AMPK in muscle have mildly decreased  $+dP/dt$  and  $-dP/dt$  under normoxic conditions and develop more pronounced cardiac dysfunction than wild-type mice under low-flow ischemia. In our experiments, perfusion with 2  $\mu$ M DXR, which already downregulated AMPK, also affected  $-dP/dt$  and LVEDP, whereas CF remained unchanged. In contrast, at 20  $\mu$ M DXR, reduced AMPK signaling was accompanied by a strong impairment of all functional parameters, including CF. Inhibition of the AMPK-regulating energy supply may reduce oxidative capac-

ity and subsequently diminish CF, which could cause a feedback potentiating cardiac injury.

Cytotoxic effects of DXR, which are fatal for the heart, could be important for its anticancer action. Both compromised CK and AMPK signaling can sensitize cancer cells for energetic or nutrient shortage and thus facilitate their apoptotic elimination. In fact, a decrease in the AMPK protein level by antisense RNA was shown to inhibit tumor growth in a mouse model by reducing the tolerance of cancer cells to nutrient starvation (21). In contrast, tumors overexpressing the uMtCK isoenzyme, which is less DXR sensitive than heart sMtCK, are renowned for their resistance to chemotherapy (1).

Taken together, our results suggest that acute cardiac dysfunction caused by clinically relevant DXR concentrations may involve impaired energy signaling via AMPK. This would be consistent with a fast inhibition of fatty acid oxidation and only transient stimulation of glucose uptake that was observed after DXR treatment (2, 14). The CK system, despite some defects, seems to maintain its functionality under acute conditions, partially because of a compensation between isoenzymes. In contrast, as suggested by our previous study (44), substantial direct and radical-mediated molecular damage of CK will accumulate with time, including inactivation of CK isoenzymes and further impairment of sMtCK functions. Such long-term CK damage could be at the origin of numerous deleterious processes that promote chronic DXR-induced cardiac dysfunction (25, 45). Compromised sMtCK functions would affect energetic coupling between mitochondria and cytosol (38), destabilize mitochondrial contact sites (3), and sensitize cells to apoptosis (7). Inhibition of MCK, functionally coupled to Ca<sup>2+</sup> pumps of the sarcoplasmic reticulum, would impair Ca<sup>2+</sup> handling, which is critical for muscle contraction and relaxation (46). Microfibrillar disarray and apoptosis, both suggested as important mechanisms of DXR cardiotoxicity (24, 25), were not yet detectable in our experimental system, suggesting that the changes in kinases regulating energy supply are among the very early effects of DXR in cardiomyocytes. The accumulation of anthracyclines and their metabolites in heart tissue, in particular in nuclei and mitochondria, would lead to sustained impairment of CK and AMPK functions, which could contribute to chronic cardiotoxicity, the most serious complication of anthracycline therapy. This hypothesis warrants, however, further verification. If it turned out to be correct, components of the CK and AMPK systems may eventually become suitable targets for cardioprotective therapy.

#### ACKNOWLEDGMENTS

We gratefully acknowledge the kind gift of DXR by Pharmacia (Milan, Italy). We thank all group members for valuable advice, help, and discussions. Elisabeth Ehler and Jean-Claude Perriard are acknowledged for antibodies and helpful suggestions.

#### GRANTS

This study was supported by Swiss National Science Foundation Grants 3234-069276 (Marie Heim-Vögtlin Subsidy to M. Tokarska-Schlattner), 3200-063417.00 (to M. Zaugg), and 3200B0-103980.04 (to M. Zaugg) and grants from Schweizerische Herzstiftung (to T. Wallimann, U. Schlattner, and M. Zaugg), Wolfemann-Nägeli-Stiftung (to U. Schlattner and T. Wallimann), Schweizer Krebsliga (to U. Schlattner and T. Wallimann), Zentralschweizer Krebsstiftung (to U. Schlattner and T. Wallimann), and Swiss University Conference (to M. Zaugg and M. C. Schaub).

## REFERENCES

1. **Bold RJ, Termuhlen PM, and McConkey DJ.** Apoptosis, cancer and cancer therapy. *Surg Oncol* 6: 133–142, 1997.
2. **Bordoni A, Biagi P, and Hrelia S.** The impairment of essential fatty acid metabolism as a key factor in doxorubicin-induced damage in cultured rat cardiomyocytes. *Biochim Biophys Acta* 1440: 100–106, 1999.
3. **Brdiczka D, Beutner G, Ruck A, Dolder M, and Wallimann T.** The molecular structure of mitochondrial contact sites. Their role in regulation of energy metabolism and permeability transition. *Biofactors* 8: 235–242, 1998.
4. **Carling D.** The AMP-activated protein kinase cascade—a unifying system for energy control. *Trends Biochem Sci* 29: 18–24, 2004.
5. **Cheneval D, Carafoli E, Powell GL, and Marsh D.** A spin-label electron spin resonance study of the binding of mitochondrial creatine kinase to cardiolipin. *Eur J Biochem* 186: 415–419, 1989.
6. **DeAtley SM, Aksenov MY, Aksenova MV, Jordan B, Carney JM, and Butterfield DA.** Adriamycin-induced changes of creatine kinase activity in vivo and in cardiomyocyte culture. *Toxicology* 134: 51–62, 1999.
7. **Dolder M, Walzel B, Speer O, Schlattner U, and Wallimann T.** Inhibition of the mitochondrial permeability transition by creatine kinase substrates. Requirement for microcompartmentation. *J Biol Chem* 278: 17760–17766, 2003.
8. **Eidenschink AB, Schroter G, Muller-Weihrich S, and Stern H.** Myocardial high-energy phosphate metabolism is altered after treatment with anthracycline in childhood. *Cardiol Young* 10: 610–617, 2000.
9. **Gewirtz DA.** A critical evaluation of the mechanisms of action proposed for the antitumor effects of the anthracycline antibiotics adriamycin and daunorubicin. *Biochem Pharmacol* 57: 727–741, 1999.
10. **Hardie DG.** AMP-activated protein kinase: a master switch in glucose and lipid metabolism. *Rev Endocr Metab Disord* 5: 119–125, 2004.
11. **Hardie DG and Carling D.** The AMP-activated protein kinase—fuel gauge of the mammalian cell? *Eur J Biochem* 246: 259–273, 1997.
12. **Hochachka PW.** The metabolic implications of intracellular circulation. *Proc Natl Acad Sci USA* 96: 12233–12239, 1999.
13. **Horestein MS, Vander Heide RS, and L’Ecuyer TJ.** Molecular basis of anthracycline-induced cardiotoxicity and its prevention. *Mol Genet Metab* 71: 436–444, 2000.
14. **Hrelia S, Fiorentini D, Maraldi T, Angeloni C, Bordoni A, Biagi PL, and Hakim G.** Doxorubicin induces early lipid peroxidation associated with changes in glucose transport in cultured cardiomyocytes. *Biochim Biophys Acta* 1567: 150–156, 2002.
15. **Ingwall JS.** The hypertrophied myocardium accumulates the MB-creatine kinase isozyme. *Eur Heart J* 5, Suppl F: 129–139, 1984.
16. **Ingwall JS.** Transgenesis and cardiac energetics: new insights into cardiac metabolism. *J Mol Cell Cardiol* 37: 613–623, 2004.
17. **Ito H, Miller SC, Billingham ME, Akimoto H, Torti SV, Wade R, Gahlmann R, Lyons G, Kedes L, and Torti FM.** Doxorubicin selectively inhibits muscle gene expression in cardiac muscle cells in vivo and in vitro. *Proc Natl Acad Sci USA* 87: 4275–4279, 1990.
18. **Jain D.** Cardiotoxicity of doxorubicin and other anthracycline derivatives. *J Nucl Cardiol* 7: 53–62, 2000.
19. **Jeyaseelan R, Poizat C, Wu HY, and Kedes L.** Molecular mechanisms of doxorubicin-induced cardiomyopathy. Selective suppression of Reiske iron-sulfur protein, ADP/ATP translocase, and phosphofructokinase genes is associated with ATP depletion in rat cardiomyocytes. *J Biol Chem* 272: 5828–5832, 1997.
20. **Joubert F, Mateo P, Gillet B, Beloil JC, Mazet JL, and Hoerter JA.** CK flux or direct ATP transfer: versatility of energy transfer pathways evidenced by NMR in the perfused heart. *Mol Cell Biochem* 256–257: 43–58, 2004.
21. **Kato K, Ogura T, Kishimoto A, Minegishi Y, Nakajima N, Miyazaki M, and Esumi H.** Critical roles of AMP-activated protein kinase in constitutive tolerance of cancer cells to nutrient deprivation and tumor formation. *Oncogene* 21: 6082–6090, 2002.
22. **Kay L, Nicolay K, Wieringa B, Saks V, and Wallimann T.** Direct evidence for the control of mitochondrial respiration by mitochondrial creatine kinase in oxidative muscle cells in situ. *J Biol Chem* 275: 6937–6944, 2000.
23. **Khuchua ZA, Qin W, Boero J, Cheng J, Payne RM, Saks VA, and Strauss AW.** Octamer formation and coupling of cardiac sarcomeric mitochondrial creatine kinase are mediated by charged N-terminal residues. *J Biol Chem* 273: 22990–22996, 1998.
24. **Lim CC, Zuppinger C, Guo X, Kuster GM, Helmes M, Eppenberger HM, Suter TM, Liao R, and Sawyer DB.** Anthracyclines induce calpain-dependent titin proteolysis and necrosis in cardiomyocytes. *J Biol Chem* 279: 8290–8299, 2004.
25. **Minotti G, Menna P, Salvatorelli E, Cairo G, and Gianni L.** Anthracyclines: molecular advances and pharmacologic developments in antitumor activity and cardiotoxicity. *Pharmacol Rev* 56: 185–229, 2004.
26. **Miura T, Muraoka S, and Ogiso T.** Adriamycin-Fe<sup>3+</sup>-induced inactivation of rat heart mitochondrial creatine kinase: sensitivity to lipid peroxidation. *Biol Pharm Bull* 17: 1220–1223, 1994.
27. **Nazeyrollas P, Prevost A, Baccard N, Manot L, Devillier P, and Millart H.** Effects of amifostine on perfused isolated rat heart and on acute doxorubicin-induced cardiotoxicity. *Cancer Chemother Pharmacol* 43: 227–232, 1999.
28. **Neumann D, Schlattner U, and Wallimann T.** A molecular approach to the concerted action of kinases involved in energy homeostasis. *Biochem Soc Trans* 31: 169–174, 2003.
29. **Nicolay K, Aue WP, Seelig J, van Echteld CJ, Ruigrok TJ, and de Kruijff B.** Effects of the anti-cancer drug adriamycin on the energy metabolism of rat heart as measured by in vivo <sup>31</sup>P-NMR and implications for adriamycin-induced cardiotoxicity. *Biochim Biophys Acta* 929: 5–13, 1987.
30. **Nicolay K and de Kruijff B.** Effects of adriamycin on respiratory chain activities in mitochondria from rat liver, rat heart and bovine heart. Evidence for a preferential inhibition of complex III and IV. *Biochim Biophys Acta* 892: 320–330, 1987.
31. **Olson RD and Mushlin PS.** Doxorubicin cardiotoxicity: analysis of prevailing hypotheses. *FASEB J* 4: 3076–3086, 1990.
32. **Pelikan PC, Gerstenblith G, Vandegaer K, and Jacobus WE.** Absence of acute doxorubicin-induced dysfunction of heart mitochondrial oxidative phosphorylation and creatine kinase activities. *Proc Soc Exp Biol Med* 188: 7–16, 1988.
33. **Pelikan PC, Weisfeldt ML, Jacobus WE, Miceli MV, Bulkley BH, and Gerstenblith G.** Acute doxorubicin cardiotoxicity: functional, metabolic, and morphologic alterations in the isolated, perfused rat heart. *J Cardiovasc Pharmacol* 8: 1058–1066, 1986.
34. **Ponticos M, Lu QL, Morgan JE, Hardie DG, Partridge TA, and Carling D.** Dual regulation of the AMP-activated protein kinase provides a novel mechanism for the control of creatine kinase in skeletal muscle. *EMBO J* 17: 1688–1699, 1998.
35. **Rajagopalan S, Politi PM, Sinha BK, and Myers CE.** Adriamycin-induced free radical formation in the perfused rat heart: implications for cardiotoxicity. *Cancer Res* 48: 4766–4769, 1988.
36. **Russell RR III, Li J, Coven DL, Pypaert M, Zechner C, Palmeri M, Giordano FJ, Mu J, Birnbaum MJ, and Young LH.** AMP-activated protein kinase mediates ischemic glucose uptake and prevents postischemic cardiac dysfunction, apoptosis, and injury. *J Clin Invest* 114: 495–503, 2004.
37. **Schlattner U, Eder M, Dolder M, Khuchua ZA, Strauss AW, and Wallimann T.** Divergent enzyme kinetics and structural properties of the two human mitochondrial creatine kinase isoenzymes. *Biol Chem* 381: 1063–1070, 2000.
38. **Schlattner U, Forstner M, Eder M, Stachowiak O, Fritz-Wolf K, and Wallimann T.** Functional aspects of the X-ray structure of mitochondrial creatine kinase: a molecular physiology approach. *Mol Cell Biochem* 184: 125–140, 1998.
39. **Schlattner U, Mockli N, Speer O, Werner S, and Wallimann T.** Creatine kinase and creatine transporter in normal, wounded, and diseased skin. *J Invest Dermatol* 118: 416–423, 2002.
40. **Schlattner U and Wallimann T.** A quantitative approach to membrane binding of human ubiquitous mitochondrial creatine kinase using surface plasmon resonance. *J Bioenerg Biomembr* 32: 123–131, 2000.
41. **Singal PK, Iliskovic N, Li T, and Kumar D.** Adriamycin cardiomyopathy: pathophysiology and prevention. *FASEB J* 11: 931–936, 1997.
42. **Sokolove PM.** Interactions of adriamycin aglycones with mitochondria may mediate adriamycin cardiotoxicity. *Int J Biochem* 26: 1341–1350, 1994.
43. **Subramanian M, Jutila A, and Kinnunen PK.** Binding and dissociation of cytochrome c to and from membranes containing acidic phospholipids. *Biochemistry* 37: 1394–1402, 1998.



44. Tokarska-Schlattner M, Wallimann T, and Schlattner U. Multiple interference of anthracyclines with mitochondrial creatine kinases: preferential damage of the cardiac isoenzyme and its implications for drug cardiotoxicity. *Mol Pharmacol* 61: 516–523, 2002.
45. Ventura-Clapier R, Garnier A, and Veksler V. Energy metabolism in heart failure. *J Physiol* 555: 1–13, 2004.
46. Wallimann T, Wyss M, Brdiczka D, Nicolay K, and Eppenberger HM. Intracellular compartmentation, structure and function of creatine kinase isoenzymes in tissues with high and fluctuating energy demands: the 'phosphocreatine circuit' for cellular energy homeostasis. *Biochem J* 281: 21–40, 1992.
47. Wallimann T, Zurbriggen B, and Eppenberger HM. Separation of mitochondrial creatine kinase (MiMi-CK) from cytosolic creatine kinase isoenzymes by Cibachrome-blue affinity chromatography. *Enzyme* 33: 226–231, 1985.
48. Weinstein DM, Mihm MJ, and Bauer JA. Cardiac peroxynitrite formation and left ventricular dysfunction following doxorubicin treatment in mice. *J Pharmacol Exp Ther* 294: 396–401, 2000.
49. Wyss M and Kaddurah-Daouk R. Creatine and creatinine metabolism. *Physiol Rev* 80: 1107–1213, 2000.
50. Wyss M, Schlegel J, James P, Eppenberger HM, and Wallimann T. Mitochondrial creatine kinase from chicken brain. Purification, biophysical characterization, and generation of heterodimeric and heterooctameric molecules with subunits of other creatine kinase isoenzymes. *J Biol Chem* 265: 15900–15908, 1990.
51. Ye Y, Wang C, Zhang J, Cho YK, Gong G, Murakami Y, and Bache RJ. Myocardial creatine kinase kinetics and isoform expression in hearts with severe LV hypertrophy. *Am J Physiol Heart Circ Physiol* 281: H376–H386, 2001.
52. Zhang J. Myocardial energetics in cardiac hypertrophy. *Clin Exp Pharmacol Physiol* 29: 351–359, 2002.
53. Zhou S, Starkov A, Froberg MK, Leino RL, and Wallace KB. Cumulative and irreversible cardiac mitochondrial dysfunction induced by doxorubicin. *Cancer Res* 61: 771–777, 2001.
54. Zou MH, Hou XY, Shi CM, Kirkpatrick S, Liu F, Goldman MH, and Cohen RA. Activation of 5'-AMP-activated kinase is mediated through c-Src and phosphoinositide 3-kinase activity during hypoxia-reoxygenation of bovine aortic endothelial cells. Role of peroxynitrite. *J Biol Chem* 278: 34003–34010, 2003.
55. Zou MH, Kirkpatrick SS, Davis BJ, Nelson JS, Wiles WG IV, Schlattner U, Neumann D, Brownlee M, Freeman MB, and Goldman MH. Activation of the AMP-activated protein kinase by the anti-diabetic drug metformin in vivo. Role of mitochondrial reactive nitrogen species. *J Biol Chem* 279: 43940–43951, 2004.

